

Molecular Structure of Free Molecules of the Fullerene C₇₀ from Gas-Phase Electron Diffraction

Kenneth Hedberg,^{*,†} Lise Hedberg,[†] Michael Bühl,[‡] Donald S. Bethune,[§]
C. A. Brown,[§] and Robert D. Johnson^{§,⊥}

Contribution from the Department of Chemistry, Oregon State University, Corvallis, Oregon 97331-4003, Organisch-Chemisches Institut, Universität Zürich, Winterthurerstrasse 190, CH-8057 Zürich, Switzerland, and IBM Research Division, Almaden Research Center, 650 Harry Road, San Jose, California 95120-6099

Received January 15, 1997[⊗]

Abstract: Electron-diffraction patterns of the fullerene C₇₀ in the gaseous state at 810–835 °C have been recorded in experiments similar to those recently described for C₆₀. The radial distribution curve calculated from the scattered intensity is entirely consistent with a molecule of *D*_{5h} symmetry. With assumption of this symmetry, 12 parameters are required to specify the structure. Reliable values are thus much more difficult to obtain for these parameters than for C₆₀ whose structure is completely defined by only two parameters. Six different models were found that give excellent fits to the diffraction data. The models may be divided into two types characterized either by a shorter (1.4+ Å) or a longer (1.5+ Å) equatorial bond. Despite this difference, however, the *average* length of the eight bonds is similar in all models (1.434 Å; average deviation 0.006 Å). Since no model could be favored on the basis of the electron-diffraction data alone, a best model was selected from considerations of theoretical energies (BP86/TZP level of density functional theory) and by comparison of computed ¹³C NMR chemical shifts (gauge-including atomic orbitals, GIAO-SCF/TZP) with those from experiment. This model is in good agreement with structures determined in the crystal by neutron and X-ray diffraction, and with *ab initio* calculated structures (BP86/TZP), with one important difference: the equatorial bond is some 0.06 Å longer. Based on assumed *D*_{5h} symmetry, and designating the five circles of atoms from the top (capping) pentagon to the equator as a, b, c, d, and e, the bond lengths (*r_a*/Å) are as follows: *r*(a–a) = 1.461(8), *r*(a–b) = 1.388(16), *r*(b–c) = 1.453(11), *r*(c–c) = 1.386(25), *r*(c–d) = 1.468(11), *r*(d–d) = 1.425(14), *r*(d–e) = 1.405(13), *r*(e–e) = 1.538(19). The equatorial diameter of the ellipsoid is 7.178(50) Å, and the distance between the polar pentagons is 7.906(64) Å; quantities in parentheses are 2 esd.

Introduction

Five years ago we reported¹ a determination of the structure of the fullerene C₆₀ based on an analysis of gas-phase electron-diffraction data (GED) at 700 °C. The determination was straightforward because of the high (icosahedral) symmetry of the molecule: the 1770 individual interatomic distances have but 23 different values, and the structure is completely specified by only two of them, for example the two different types of bonds.

The structure of the molecule C₇₀ (Figure 1) presents a much more difficult problem. The insertion of ten additional atoms into C₆₀ in the form of an equatorial belt reduces the symmetry of the resulting C₇₀ to *D*_{5h}, increases the number of individual distances to 2415 (which have 143 different values), and requires the values of 12 geometrical parameters to define the structure. Shortly after our C₆₀ study we obtained photographic diffraction data from a sample of C₇₀, which we analyzed in similar fashion. However, one of the preliminary bond-length results—that between atoms of the equatorial belt—seemed implausibly large at 1.55–1.59 Å compared to an *ab initio* value (SCF/dzp) of about 1.48 Å.² Since a few of these C₇₀ plates (those with

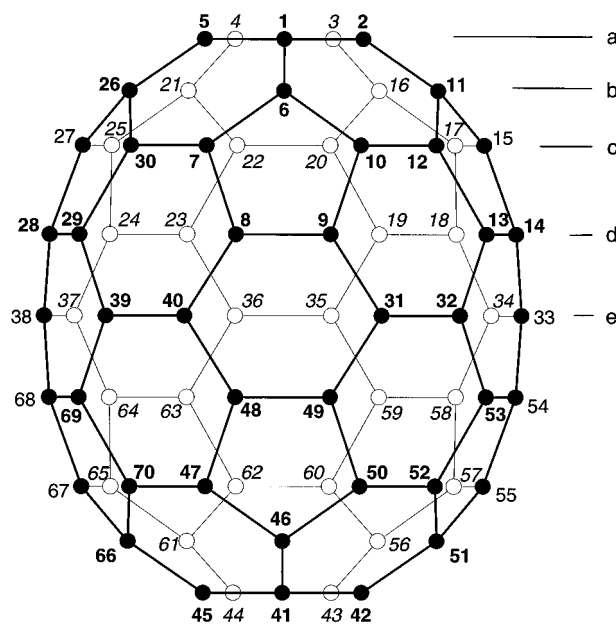


Figure 1. Diagram of the *D*_{5h} symmetry C₇₀ molecule with atom numbering. There are five types of atoms indicated by the lower case letters.

higher-angle data) were quite light compared to the C₆₀ ones, it was conceivable that the value of the suspect distance had been unreliably measured. It was desirable to repeat the higher-angle experiments in an attempt to obtain darker plates, which might improve the signal-to-noise ratio and remove this aspect of

[†] Oregon State University.

[‡] Organisch-Chemisches Institut.

[§] IBM Research Division.

[⊥] Present address: IBM Watson Research Center, P.O. Box 704, M.S. J1-N54, Yorktown Heights, NY 10598.

[⊗] Abstract published in *Advance ACS Abstracts*, May 15, 1997.

(1) Hedberg, K.; Hedberg, L.; Bethune, D. S.; Brown, C. A.; Dorn, H. C.; Johnson, R. D.; deVries, M. *Science* **1991**, *254*, 410.

(2) Scuseria, G. *Chem. Phys. Lett.* **1991**, *180*, 451.

uncertainty about the equatorial bond distance. The experiments have now been done with a different C₇₀ sample and with improved shielding of the high-temperature oven.³ However, although the photographic plates from these new experiments are indeed of higher optical density than the earlier ones, the structural results from the two experiments are similar.

In the period following our first experiments on it, the structure of C₇₀ has been investigated in the solid state by electron diffraction⁴ and neutron diffraction,⁵ and in the form of the adduct C₇₀S₄₈, by X-ray diffraction.⁶ There have also been a number of semiempirical and ab initio MO studies.⁷ In each of these experimental and theoretical investigations the length of the equatorial bond was found to be less than 1.49 Å. Our now completed analysis of the gas-phase structure of the molecule has led to six different models in good agreement with the electron-diffraction data, some of which have an equatorial bond length similar to the solid state and theoretical values. We have not been able to select a "best model" on the basis of the GED data. However, we also carried out ab initio calculations of relative energies and NMR chemical shifts for these models. Chemical shifts are often particularly useful in model choices because they are structure sensitive and can be compared with experimental shifts from an independent source. For example, GED geometries of a number of complex polyhedral heteroboranes have been selected or corroborated on the basis of such ab initio/NMR criteria.⁸ Judged from these calculations on C₇₀, the best of our GED models has an equatorial bond length r_a equal to 1.538(19) Å.⁹ The following is a report of our results.

Experimental Section

The first C₇₀ sample was obtained as one of the components from a fullerene generator. Its preparation and purification were as described earlier.¹ The second sample was a commercial one of high purity. The diffraction experiments were carried out in a way similar to that described for C₆₀.¹ The behavior of the sample was also similar to that described for C₆₀, but at 825 °C the oven temperature required to obtain sufficient scattering from the emerging gas was about 100 °C hotter. Even so, there was no evidence of decomposition at this temperature: scrapings from the oven after one experiment yielded identical diffraction patterns in subsequent experiments. Parameters for the diffraction experiments were as follows: rotating sector, angular opening proportional to r^3 ; nominal accelerating voltage, 60 kV; voltage calibration, separate diffraction experiments against CS₂ ($C=S = 1.577$ Å and $S \cdots S = 3.109$ Å); photographic plates, 8 × 10 in. Kodak projector slide medium contrast; development, 10 min in D19 diluted 1 × 1; nominal camera distances, 750 (LC) and 300 mm (MC). A total of 11 plates, three LC and six MC from the first sample and two

(3) Although the high-temperature oven as a whole was shielded to prevent light exposure of the photographic plates, the darkening of the plates from the glowing nozzle tip was more severe with C₇₀ than with C₆₀.

(4) McKenzie, D. R.; Davis, C. A.; Cockayne, D. J. H.; Muller, D. A.; Vassallo, A. M. *Nature* **1992**, *355*, 622.

(5) Nikolaev, A. V.; Dennis, T. J. S.; Prassides, K.; Soper, A. K. *Chem. Phys. Lett.* **1994**, *223*, 143.

(6) Roth, G.; Adelman, P. J. *Phys. I* **1992**, *2*, 1541.

(7) Summarized in: Cioslowski, J. *Electronic Structure Calculations on Fullerenes and Their Derivatives*; Oxford University Press: New York, 1992; Chapter 4.

(8) For example, see the following and references cited therein. (a) Hnyk, D.; Hofmann, M.; Schleyer, P. V. R.; Bühl, M.; Rankin, D. W. H. *J. Phys. Chem.* **1996**, *100*, 3434. (b) Brain, P. T.; Rankin, D. W. H.; Robertson, H. E.; Greatrex, R.; Fox, M. A.; Nikrahi, A.; Bühl, M. *Inorg. Chem.* In press.

(9) Distance types used in the present work are r_a , the distance between average atomic positions (the set of r_a is consistent with D_{5h} symmetry), r_g , the thermal average distance, and r_a , the quantity measured directly from GED interference functions. The relationships are $r_g = r_a + \delta r + K$ and $r_a = r_g - l^2/r$, where δr and K are small corrections for centrifugal distortion and harmonic vibration, and l^2 is a mean square vibrational amplitude. See: Kuchitsu, K.; Cyvin, S. J. In *Molecular Structures and Vibrations*; Cyvin, S. J., Ed.; Elsevier: Amsterdam, 1972; Chapter 12.

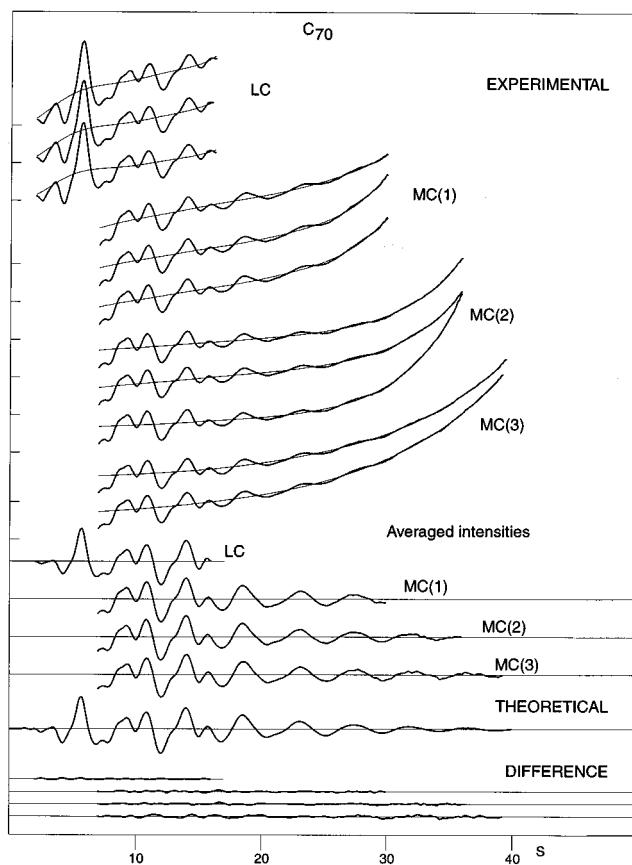


Figure 2. Intensity curves. Long-camera and middle-camera experimental curves are magnified 2.5 times relative to the backgrounds on which they are superimposed in order to show the undulations better. Averaged curves are in the form $sI_M(s)$. The theoretical curve is for model Cb. Difference curves are experimental minus theoretical.

MC from the second, were selected for data analysis. The procedures have been described.^{10,11} Tabulated values of complex electron-scattering factors¹² were used in these and other subsequent procedures. Ranges of the averaged intensity data from each experiment were $2.00 \leq s/\text{Å}^{-1} \leq 16.00$ (first sample, LC), $7.00 \leq s/\text{Å}^{-1} \leq 30.00$ (first sample, MC, three plates), $7.00 \leq s/\text{Å}^{-1} \leq 36.00$ (first sample, MC, another three plates), and $7.00 \leq s/\text{Å}^{-1} \leq 39.25$ (second sample, MC). Curves of these data are shown in Figure 2; the data are available as Supporting Information.

Computational Section

Single-point energy calculations were carried out at the Hartree–Fock self-consistent field (SCF) level¹³ and at a gradient-corrected level of density functional theory (DFT),¹⁴ using Becke's 1988¹⁵ and Perdew's 1986¹⁶ exchange-correlation functionals (denoted BP86) and a medium-sized grid (grid 3).¹⁷ Magnetic shieldings were computed with the gauge-including atomic orbitals (GIAO) SCF method¹⁸ in its direct

(10) Gundersen, G.; Hedberg, K. *J. Chem. Phys.* **1969**, *51*, 2500.

(11) Hedberg, L. Abstracts, 5th Austin Symposium on Gas Phase Molecular Structure, Austin, Texas, 1974, No. 37.

(12) Ross, A. W.; Fink, M.; Hilderbrandt, R. I. *International Tables for Crystallography*; International Union of Crystallography; Kluwer: Boston, Dordrecht, London.

(13) For standard methods and basis sets see: Hehre, W. J.; Radom, L.; Schleyer, P. V. R.; Pople, J. A. *Ab initio Molecular Orbital Theory*; Wiley: New York, 1986.

(14) For example: (a) Parr, R. G.; Yang, W. *Density Functional Theory of Atoms and Molecules*; Academic Press: Oxford, 1989. (b) Seminario, J. M.; Politzer, P., Eds. *Modern Density Functional Theory*; Elsevier: Amsterdam, 1995.

(15) Becke, A. D. *Phys. Rev. A* **1988**, *38*, 3098.

(16) Perdew, J. P. *Phys. Rev. B* **1986**, *33*, 8822; **1986**, *34*, 7406.

(17) Treutler, O.; Ahlrichs, R. *J. Chem. Phys.* **1995**, *102*, 346.

(18) (a) Ditchfield, R. *Mol. Phys.* **1974**, *27*, 789. (b) Wolinski, K.; Hinton, J. F.; Pulay, P. *J. Am. Chem. Soc.* **1990**, *112*, 8251.

Table 1. Equatorial C–C Bond Lengths, Energies, and $^{13}\text{C}^a$ and Endohedral Chemical Shifts for C_{70} Models

model	$r(\text{eq})/\text{\AA}$	E_h energies – 2650.0		chemical shifts/ppm ^{a,b}					$\delta(\text{endo})^c$
		SCF/TZP	BP86/TZP	C(a)	C(b)	C(c)	C(d)	C(e)	
Aa	1.432(37)	0.91590	18.02936	151.4	149.9	147.9	141.7	124.1	–24.3
Ab	1.557(15)	0.93711	18.04693	150.6	145.8	145.9	140.5	132.1	–28.0
Ca	1.423(39)	0.91957	18.04141	150.7	145.4	149.1	142.1	124.1	–25.4
Cb	1.538(19)	0.94258	18.05747	149.3	146.8	146.2	141.8	131.8	–28.6
Ba	1.407(50)	0.82617	17.96770	142.8	164.8	147.7	139.4	125.3	–30.5
Da	1.387(47)	0.78568	17.94091	141.8	168.4	147.1	139.4	125.3	–29.0
SCF/DZP ^d	1.475	0.97598	18.05535	145.5	142.8	141.7	139.4	127.8	–28.2
BP86/TZP	1.471	0.94320	18.07761	148.8	145.7	146.1	143.8	131.6	–30.6
exptl ^e				150.1	146.8	147.5	144.8	130.3	–28.8 ^f

^a GIAO-SCF/TZP relative to TMS. ^b For carbon atom identification see Figure 1. ^c Negative magnetic shielding of the center of mass, see text. ^d Except for C(e), the absolute magnetic shieldings are very similar to those reported in ref 19 computed with virtually the same basis set and geometry. The relative shifts given here differ somewhat from those on p 102 of ref 7 because a different value for the standard was used; see Computational Details. ^e ^{13}C data from ref 21a. ^f $\delta(^3\text{He})$ of $\text{He}@C_{70}$ from ref 22.

Table 2. Relative Energies and Absolute Deviations between Computed and Experimental Chemical Shifts for C_{70} Models

model	$E_{\text{rel}}/\text{kcal}\cdot\text{mol}^{-1}$		$\Delta(\delta)/\text{ppm}$		
	SCF/TZP	BP86/TZP	$\delta^{13}\text{C}(\text{max})$	$\delta^{13}\text{C}(\text{av})$	$\delta(^3\text{He})$
Aa	37.7	30.3	6.2	2.8	4.5
Ab	24.4	19.3	4.3	1.8	0.8
Ca	35.4	22.7	6.2	2.5	3.4
Cb	21.0	12.6	3.0	1.3	0.2
Ba	94.0	69.0	18.0	7.2	1.7
Da	119.4	85.8	21.6	8.1	0.2
SCF/DZP	0.0	14.0	5.8	4.5	0.6
BP86/TZP	20.6	0.0	1.4	1.2	1.8

implementation.¹⁹ Energy and chemical shift calculations employed a [9s5p]/(5s3p) triple- ζ basis set²⁰ augmented with one set of d-polarization functions (exponent 0.8) denoted TZP. ^{13}C chemical shifts were calculated relative to C_{60} in its experimental GED geometry¹ (computed carbon shielding 38.5 ppm) and have been converted to the usual TMS scale by using the experimental ^{13}C chemical shift of C_{60} , 142.7 ppm.²¹ Endohedral chemical shifts, $\delta(\text{endo})$, were determined in terms of the negative magnetic shielding of the center of mass; these $\delta(\text{endo})$ values can be compared to the ^3He chemical shift of the corresponding endohedral He compound, $\delta(^3\text{He})$ ²² (see also the nucleus-independent chemical shift (NICS)).²³ Geometries were taken from the GED models described below (models Aa, Ab, Ca, Cb, Ba, and Da) and from earlier theoretical studies at the levels SCF/DZP² and BP86/TZP.²⁴

D_{5h} symmetry was used throughout, and all computations were done with the TURBOMOLE²⁵ program package. The results of these various calculations are summarized in Tables 1 and 2.

Structure Analysis

Radial Distribution Curves. For purposes of generating the experimental radial distribution of distances from the GED data, composite intensity curves were formulated by combining the average LC data with various averages of the MC data. We tested the MC data from the first and the second samples both separately and together. The differences were insignificant, as

(19) Häser, M.; Ahlrichs, R.; Baron, H. P.; Weiss, P.; Horn, H. *Theor. Chim. Acta* **1992**, *83*, 455.

(20) Dunning, T. H. *J. Chem. Phys.* **1979**, *53*, 2823.

(21) (a) Taylor, R.; Hare, J. P.; Abdul-Sala, A. K.; Kroto, H. W. *J. Chem. Soc., Chem. Commun.* **1990**, 1423. (b) Ajio, H.; Alvarez, M. M.; Anz, S. J.; Beck, R. D.; Diederich, F.; Fostropoulos, K.; Huffman, D. R.; Krätschmer, W.; Rubin, Y.; Shriver, K. E.; Sensharma, D.; Whetten, R. L. *J. Phys. Chem.* **1990**, *94*, 8630.

(22) Saunders, M.; Jimenez-Vazquez, H. A.; Cross, R. J.; Mroczkowski, S.; Freedberg, D.; Anet, F. A. L. *Nature* **1994**, *367*, 256.

(23) Schleyer, P. V. R.; Maerker, C.; Dransfeld, A.; Jiao, H.; Hommes, N. J. R. v. E. *J. Am. Chem. Soc.* **1996**, *118*, 6317.

(24) Bühl, M.; v. Wüllen, C. *Chem. Phys. Lett.* **1995**, *247*, 63. The BP86/TZP geometry was used in this study, but no structural details are given.

(25) Ahlrichs, R.; Bär, M.; Häser, M.; Horn, H.; Kölmel, C. *Chem. Phys. Lett.* **1989**, *162*, 165.

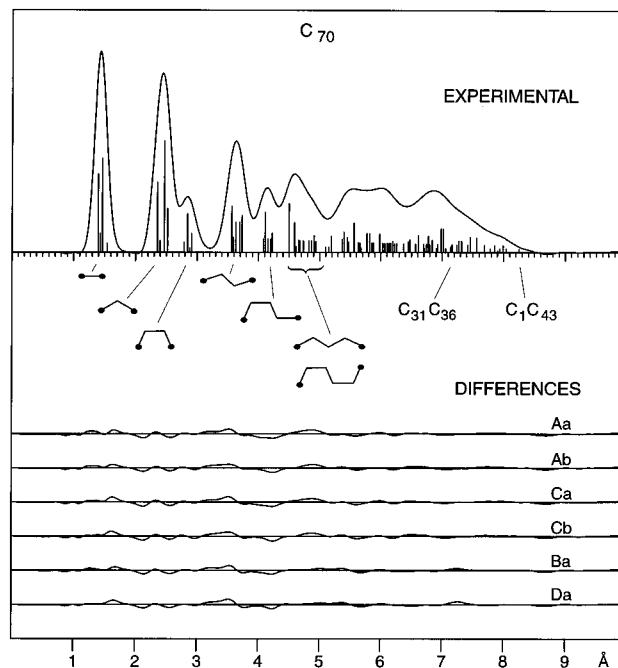


Figure 3. Radial distribution curves. Vertical bars indicate interatomic distances; lengths of bars are proportional to weights of terms. Ball-stick diagrams indicate distance types. $\text{C}_{31}\text{C}_{36}$ is the longest distance in the equatorial plane and C_1C_{43} the longest in the molecule. Differences are experimental minus theoretical for the six converged models.

were the differences between preliminary refinement results obtained from similar combinations of experimental data. The curve shown in Figure 3 is from a combination of the four average intensities shown in Figure 2. Comparison with theoretical radial distribution curves based upon plausible models of C_{70} showed the experimental data to be completely consistent with a molecule of D_{5h} symmetry. There was no evidence of thermal decomposition.

Models. The 12 independent parameters required for specification of the molecular structure of C_{70} might be taken as the 8 different bond lengths and 4 interbond angles. However, for programmatic purposes it was more convenient to choose a parameter set that comprised a pair of bond lengths, several bond-length differences, some angles (interbond, out-of-plane, “flap”), the radius of the ellipsoid, and the length of the major axis. The members of this set are as follows and may be identified by reference to Figure 1: $r(\text{eq}) = r(31-32)$; $r(1-2)$; $\Delta r(1,6) = r(1-6) - r(1-2)$; $\Delta r(6,7) = r(6-7) - r(1-2)$; $\Delta r(7,8) = r(7-8) - r(1-2)$; $\Delta r(8,9) = r(8-9) - r(1-2)$; $\angle(7-6-10)$; OOP(1,6) is the out-of-plane displacement of bond $r(1-6)$ from the pentagon on the 5-fold axis; OOP(6,1) is the out-

of-plane displacement of bond $r(6-1)$ from the plane defined by atoms 7,6,10; FLAP is the angle between the planes defined by atoms 7,6,10 and 7,8,9,10; RR-EQ is the distance from the center of the molecule to one of the equatorial atoms; and Z is the distance along the major axis from the center of the molecule to the plane of a capping five-member ring. In addition to these geometrical parameters it is necessary to take account of the nonrigidity of the molecule by specification of vibrational amplitude parameters associated with pairs of atoms—in principle, one for each of the 143 different interatomic distances. To reduce these 143 separate quantities to a manageable number, they were combined in the usual way into several groups, each of which was defined by a group-amplitude parameter. Amplitude values for members of a group thus changed in the course of refinement, but differences between them remained fixed.

The definition of C_{70} models for refinement requires more than the specification of parameters; their modes of handling must also be decided. Most important, the number of geometrical parameters (12) is much too large to be refined with each taken as an independent entity,²⁶ and accordingly simplifying assumptions and/or constraints for these parameters are necessary. Further, a well-known complication in the analysis of molecular structures by gas-phase electron diffraction (GED) is the effect of vibration on distance values. This vibrational averaging effect, often termed “shrinkage”,²⁷ generally leads to average distances that are not totally consistent with equilibrium molecular symmetry. Although corrections for vibrational averaging are normally not difficult to calculate with use of a normal-coordinate program, they are enormously more so in the case of a large molecule like C_{70} and have not been carried out; thus, assumptions about such corrections have to be made. Other decisions concern refinement of the vibrational amplitudes themselves. Although their number can be reduced via the group-amplitude method mentioned above, assumptions about the relative values of group members must still be made. Yet another decision involves the relative weighting of the experimental intensity data—long camera versus middle camera and data from the older experiments versus the newer ones. The approach to these problems is described in the next section.

Refinements. A number of different models were tested in a series of preliminary refinements that made use of the older and the newer data separately with the intent of assessing the relative qualities of these data sets. The refinement conditions were all based on the assumption of D_{5h} symmetry for the molecule, but differed in the omission or inclusion of distance corrections designed to take account of the effects of vibrational averaging and in the use or nonuse of constraints in the form of “predicate” values.²⁸ The vibrational corrections were estimated with the help of results that are available for C_{60} .²⁹ Assignment of a predicate value allows refinement of the parameter to which it is attached, while operating as a kind of flexible tether to impede an increasing difference between the refined and assigned values. We drew our predicate values from the results of ab initio calculations² at the SCF/DZP level and assigned “uncertainties” (which in our least-squares program are used to determine the weighting³⁰) in accord with our experience in other cases. Toward the end of our work we also

used predicates drawn from the theoretical structure obtained at the BP86/TZP²⁴ level.

The most important results of these preliminary refinements may be summarized as follows. First, the parameter values obtained from the newer and the older data were not significantly different. Second, the fits to both the newer and older data were generally very good. Third, in most of the refinements characterized by a given set of conditions (*i.e.*, use of vibrational corrections and the new data only) two different converged structures were found, which were distinguished most notably by the length of the equatorial bond $r(\text{eq})$: this bond tended to be either rather large at ca. 1.55 Å or much smaller at ca. 1.44 Å. Lastly, the results for each converged structure were not strongly affected by vibrational corrections, nor by the choice of predicate values, but they were somewhat sensitive to the relative weighting of the intensity data from the low- and high-scattering angles (LC *vs* MC plates). We concluded that because results from comparable refinements using the old and new data were similar, the remaining work should be done with use of both data sets.

It is common knowledge that multiparameter spaces such as that for C_{70} may include several stable minima, and that in such cases different converged results will derive from different choices of trial structures and refinement conditions. It was not practicable to explore this possibility very thoroughly, but in view of the preliminary results cited above an investigation based on starting models with different stationary values of $r(\text{eq})$ was indicated. We carried out a large number of refinements in which all geometrical parameters were allowed to vary subject to a selected, fixed value for $r(\text{eq})$. These $r(\text{eq})$ values were chosen at intervals of 0.02 Å in the range $1.32 \leq r(\text{eq})/\text{Å} \leq 1.62$. The experimental intensity data from each of the two camera distances for the older and newer samples were formed into four separate sets of average intensities (older data: LC, MC smaller angle range, MC larger angle range; newer data: MC). There were four series of refinements based on the inclusion or exclusion of the ab initio based predicate values and of distance corrections, the latter estimated from C_{60} as before. Curves showing the quality of the fits obtained in these series are seen in Figure 4 and are revealing in two important respects. One is the quality of agreement from each of the refinements, which is quite good (between 4.5 and 6.0%), but the agreement for refinements carried out without predicates is slightly better than that with predicates. The other is that each curve has more than one actual or incipient minimum: two in A, one in B, two or three in C, and one or two in D. (In series B there appear to be two minima, but although the curve drops off at large $r(\text{eq})$, the refinements beyond $r(\text{eq}) = 1.60$ Å could not be made to converge.) Finally, we carried out refinements of trial structures close to the minima of each curve to obtain values and uncertainties for all geometrical and vibrational parameters. The refinement results for the geometrical parameters are shown in Table 3.

Selection of a Preferred Model. The choice of the best model for C_{70} from the GED data is not straightforward. It does appear that the constraints imposed by inclusion of the predicate values lead to slightly poorer agreement with experiment (*i.e.*, larger R factors) regardless of distance corrections for the effects of molecular vibration; this is evident from comparison of the curves of Figure 4 or the R factors of Table

(26) Determination of parameter values depends on the accuracy of distance measurements. The many distances in C_{70} overlap extensively, giving rise to high correlations among them that prevent accurate measurement.

(27) Bastiansen, O.; Trætteberg, M. *Acta Crystallogr.* **1960**, *13*, 1108.

(28) Bartell, L. S. In *Molecular Structure by Diffraction Methods*; Specialist Periodical Reports, Vol. 5, Chapter 4, The Chemical Society: London, 1975.

(29) Brunvoll, J. Personal communication.

(30) These uncertainties are dimensionally similar to the parameters with which they are associated, but their magnitudes have little to do with the true uncertainties of the predicates. The choice of magnitudes is determined by the desired restriction of parameter-value movement and by the way that the predicate values are handled by the least-squares program for refinement.

Table 3. Refined Parameter Values for Refined Models of $C_{70}^{a,b}$

parameter ^d	predicates ^c		with predicates				without predicates	
	value	uncer ^e	Cb ^f	Aa	Ab	Ca	Ba	Da
$r(\text{eq})$	1.475	0.0032	1.538(19)	1.432(37)	1.557(15)	1.423(39)	1.407(50)	1.387(47)
$r(1,2)$			1.461(8)	1.464(7)	1.460(7)	1.465(8)	1.425(29)	1.429(29)
$\Delta r(1,6)$	-0.076	0.001	-0.073(14)	-0.071(13)	-0.072(13)	-0.071(14)	-0.024(59)	-0.021(65)
$\Delta r(6,7)$	-0.005	0.001	-0.008(15)	-0.027(12)	-0.008(13)	-0.021(13)	0.097(29)	0.094(29)
$\Delta r(7,8)$	0.006	0.001	0.007(13)	0.039(9)	0.010(12)	0.027(11)	-0.005(29)	-0.004(31)
$\Delta r(8,9)$	-0.036	0.001	-0.036(14)	-0.045(14)	-0.041(13)	-0.042(14)	0.011(86)	0.008(89)
$\angle(7,6,10)$			107.7(22)	107.5(14)	107.0(16)	107.6(16)	106.3(12)	107.4(12)
OOP(1,6)			31.5(16)	31.9(16)	31.3(15)	32.0(17)	31.1(12)	32.4(13)
OOP(6,1)			33.0(33)	34.1(33)	34.4(31)	33.1(35)	32.4(27)	29.3(31)
FLAP			-0.2(29)	-2.3(26)	-1.6(26)	-1.1(28)	2.3(24)	4.1(27)
RR-EQ			3.590(25)	3.568(27)	3.590(24)	3.565(28)	3.542(25)	3.523(29)
Z			3.953(32)	3.968(29)	3.959(28)	3.966(31)	3.971(25)	3.990(27)
R^g			0.0558	0.0525	0.0521	0.0547	0.0461	0.0509

^a Distances in angstroms: r_a for Aa, Ab, and Ba and, necessarily, r_a for Ca, Cb, and Da where distance corrections were absent; angles (\angle_a) in degrees. Uncertainties in parentheses are estimates of 2σ . ^b Model designations are those indicated by Figure 4. ^c Reference 28. ^d See text for definitions. ^e The magnitudes of these uncertainties are not related to the predicate values themselves. See ref 30. ^f Preferred model. ^g Quality-of-fit factor: $R = [\sum_i w_i \Delta_i^2 / w_i (s_i I_i(\text{obsd})^2)]^{1/2}$ with $\Delta_i = s_i I_i(\text{obsd}) - s_i I_i(\text{calcd})$.

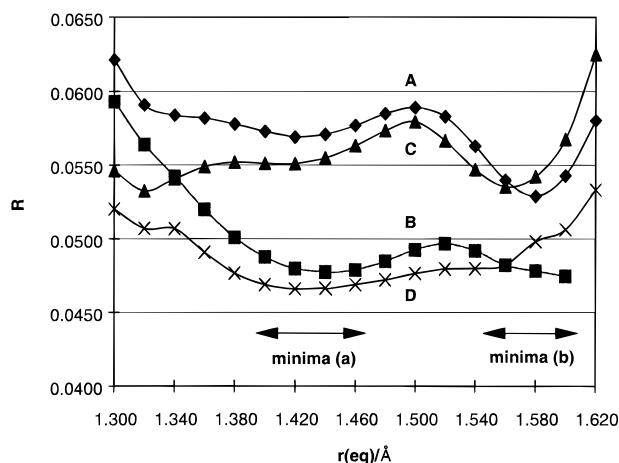


Figure 4. Curves showing the quality of fit as a function of the equatorial bond distance for refinements under various conditions. Conditions applied: curve A, both distance corrections and predicate values; curve B distance corrections only; curve C, predicate values only; curve D, neither distance corrections nor predicate values. Ranges of minima found are indicated by the arrows.

3. However, the overall agreement for all six models is excellent by usual standards, and we are inclined to give little weight to the differences in the R factors for purposes of model choice. All things considered, there is little if anything in the quality of the fits provided by the several models that allows us to rule out any of them in favor of the others. Faced with this frustrating situation we turned to the theoretical results for help.

As expected, the theoretical SCF and BP86 structures are the most stable at these levels (Table 2). Of the several GED structures, models Ba and Da, respectively about 70 and 85 kcal/mol above the minima at the BP86/TZP level, are excessively high in energy. Of the remaining models, those with the longer equatorial bonds, Ab and Cb, are lower in energy than the corresponding models with shorter bonds, Aa and Ca. One in particular, Cb, is only about 13 kcal/mol above the BP86/TZP structure and is comparable to the relative energy of the SCF/DZP structure. Given that model Cb has the five equatorial bonds about 0.07 Å longer than this theoretical model, the 13 kcal/mol energy difference does not seem very large. Turning to the chemical shifts, the experimental ^{13}C NMR spectrum consists of four signals in the relatively narrow range between about 150 and 145 ppm and a single resonance at about 130 ppm.²¹ Except for Ba and Da, qualitatively similar patterns are computed for the C_{70} models of our study. For Ba and Da

unusually large deshieldings are apparent (Table 1) for the resonances of the b-type carbon atoms which are shifted to higher frequency relative to experiment by up to 22 ppm. This deshielding, as well as the high relative energies of these models, can be attributed to the very long bonds between b- and c-type carbon atoms—some 0.07 Å longer than that calculated for the BP86/TZP structure. Of the other four models, Ab and Cb provide the best fits as judged from the deviations from experiment ($\Delta(\delta)$) seen in Table 2 and by comparison to experiment of the chemical shifts themselves seen in Table 1. Indeed, the fit to the latter provided by model Cb (average deviation from experiment of less than 2 ppm) is nearly as good as that of the best theoretical structure, BP86/TZP (average deviation 1 ppm). Note, however, that between model Cb and the theoretical BP86/TZP one, only the latter correctly reproduces the relative sequence of all five ^{13}C NMR signals.

The endohedral chemical shifts of the centers of mass, $\delta(\text{endo})$, found in Table 1 can be directly compared to the experimental ^3He chemical shift of He@ C_{70} .²² Both $\delta(\text{endo})$ and $\delta(^3\text{He})$ are largely determined by the ring currents in the fullerene cage³¹ and have been shown to be practically identical when computed at the same level.²⁴ The calculated endohedral chemical shift of C_{60} has proven to be quite sensitive to the bond lengths employed, and values of about -4 to -13 ppm (experimental: -6.3 ppm²²) have been obtained.³² Similar variations are apparent in the $\delta(\text{endo})$ values for C_{70} which range from about -24 to -31 ppm, with the experimental value at -28.8 ppm. The best agreement with the theoretical value for $\delta(\text{endo})$ is given by models Da and Cb.

From the theoretical calculations outlined above we are able to conclude the following. Models Ba and Da can be safely ruled out because of their high energies relative to the others and because of the large differences between the ^{13}C chemical shifts calculated for them and those observed.²¹ Of the remaining four models, Cb gives the best agreement between computed chemical shifts and experiment—indeed, as good as is given by the better (BP86/TZP) of the theoretical structures. This is surprising since, as we have noted, these structures differ by about 0.07 Å in the length of the equatorial bond. Apparently the computed chemical shifts, including those of the equatorial carbon atoms C(e), are not very sensitive to this parameter. Table 4 contains the r_a values of the bond distances and \angle_a values

(31) For example, see: (a) Pasquerello, A.; Schlüter, M.; Haddon, R. C. *Science* **1992**, 257, 1660. (b) Pasquerello, A.; Schlüter, M.; Haddon, R. C. *Phys. Rev. A* **1993**, 47, 1783.

(32) Bühl, M.; Thiel, W.; Jiao, H.; Schleyer, P. V. R.; Saunders, M.; Anet, F. A. L. *J. Am. Chem. Soc.* **1994**, 116, 6005.

Table 4. Selected Distances ($r_a/\text{\AA}$) and Angles (\angle/deg) from Refinements of Models of C_{70a}

parameter	calcd ^b	with predicates				without predicates	
		Cb ^c	Aa	Ab	Ca	Ba	Da
distances ^d							
C ₁ –C ₂	1.451	1.461(8)	1.467(7)	1.464(7)	1.465(8)	1.428(29)	1.428(29)
C ₆ –C ₇	1.446	1.453(11)	1.440(9)	1.455(10)	1.443(10)	1.525(7)	1.522(9)
C ₇ –C ₈	1.457	1.468(11)	1.506(6)	1.473(10)	1.492(8)	1.423(22)	1.423(26)
C ₈ –C ₉	1.415	1.425(14)	1.422(14)	1.423(13)	1.423(14)	1.425(14)	1.436(68)
C ₁ –C ₆	1.375	1.388(16)	1.385(14)	1.392(14)	1.394(15)	1.388(16)	1.407(39)
C ₁₀ –C ₁₂	1.361	1.386(25)	1.389(20)	1.389(19)	1.392(22)	1.386(25)	1.341(14)
C ₉ –C ₃₁	1.407	1.405(13)	1.411(13)	1.401(12)	1.413(14)	1.405(13)	1.448(22)
C ₃₁ –C ₃₂ ^e	1.475	1.538(19)	1.435(37)	1.560(15)	1.423(39)	1.538(19)	1.386(47)
RR–EQ ^f		3.589(25)	3.568(27)	3.590(24)	3.565(28)	3.589(25)	3.523(29)
Z ^g		3.953(32)	3.968(29)	3.959(27)	3.966(31)	3.953(32)	3.990(27)
bond angles							
$\angle(2-1-6)$		120.1(6)	119.9(6)	120.1(5)	119.9(6)	120.1(6)	119.7(5)
$\angle(1-6-7)$		119.6(14)	119.3(3)	119.4(12)	119.6(14)	119.6(14)	121.1(9)
$\angle(6-7-8)$		107.8(17)	108.8(11)	108.4(13)	108.5(13)	107.8(17)	105.3(11)
$\angle(6-7-30)$		120.3(10)	120.7(9)	120.4(8)	120.4(9)	120.3(10)	119.2(6)
$\angle(8-7-30)$		119.7(7)	119.4(6)	119.7(6)	119.4(7)	119.7(7)	120.9(10)
$\angle(7-8-9)$		108.3(8)	107.4(6)	108.1(6)	107.7(6)	108.3(8)	110.9(11)
$\angle(7-6-10)$		107.7(22)	107.5(14)	107.0(16)	107.6(16)	106.3(12)	107.4(12)
$\angle(7-8-40)$		122.4(9)	120.0(11)	122.6(8)	120.0(11)	122.4(9)	119.4(26)
$\angle(9-8-40)$		121.1(8)	123.0(9)	122.6(8)	122.8(9)	121.1(8)	121.2(15)
$\angle(8-40-39)$		117.6(7)	120.5(8)	117.4(5)	120.5(9)	117.6(7)	119.3(17)
$\angle(8-40-48)$		117.0(15)	112.5(16)	117.3(13)	112.6(17)	117.0(15)	115.8(32)
out-of-plane angles ^h							
$\angle(1-6;2,1,5)$		31.5(16)	31.9(16)	31.3(15)	32.0(17)	31.5(16)	32.4(13)
$\angle(6-1;7,6,10)$		33.0(33)	34.1(33)	34.4(31)	33.1(35)	33.0(33)	29.3(31)
flap/envelope angles ^{i,j}							
$\angle(6\bullet\bullet 11)$		0.9(27)	1.4(27)	2.0(26)	0.8(29)	0.9(27)	-1.5(24)
$\angle(7\bullet\bullet 10)$		-0.2(29)	-2.3(26)	-1.6(26)	-1.1(28)	-0.2(29)	4.1(27)
$\angle(9\bullet\bullet 13)$		-6.0(19)	-4.3(20)	-5.7(18)	-4.5(21)	-6.0(19)	-7.0(18)
$\angle(40\bullet\bullet 31)$		-10.4(23)	-15.6(28)	-9.9(21)	-16.0(29)	-10.4(23)	-16.2(33)
$\angle(31\bullet\bullet 32)$		31.6(24)	30.6(28)	31.8(23)	30.1(29)	29.9(22)	27.4(27)

^a Model designations are those indicated by Figure 4. ^b Ab initio values (ref 2) corrected to r_a . ^c Preferred model. ^d r_g values are 0.002 Å larger than the listed r_a ones. ^e Identical to parameter $r(\text{eq})$. ^f Distance from the center of the molecule to an equatorial atom. ^g Distance from the center of the molecule to a polar face. ^h Angle between the indicated bond and plane. ⁱ Bending angle of two contiguous planes around the indicated common line. ^j Positive (negative) signs indicate convex (concave) outward.

Table 5. Correlation Matrix ($\times 100$) for Geometrical Parameters of Model Cb

parameter ^a	$\sigma_{LS}^b \times 100$	r_1	r_2	r_3	r_4	r_5	r_6	\angle_7	\angle_8	\angle_9	\angle_{10}	r_{11}	r_{12}
1 $r(\text{eq})$	0.67	100	9	-4	11	-20	14	25	6	-8	4	25	-5
2 $r(1,2)$	0.27		100	-12	-70	-57	-26	33	13	10	-22	-5	1
3 $\Delta r(1,6)$	0.51			100	-1	11	5	43	3	16	-24	-17	6
4 $\Delta r(6,7)$	0.52				100	9	2	-34	-11	-7	22	2	<1
5 $\Delta r(7,8)$	0.47					100	1	-14	-2	-5	4	7	4
6 $\Delta r(8,9)$	0.51						100	-13	-5	1	<1	10	-1
7 $\angle(7,6,10)$	76.3							100	<1	-16	29	12	-46
8 OOP(1,6)	57.2								100	-81	25	12	74
9 OOP(6,1)	117									100	-75	-20	-33
10 FLAP	101										100	12	-23
11 RR–EQ	0.88											100	-23
12 Z	1.14												100

^a See test for definitions. ^b Standard deviations from least squares.

for various angles for all six refined models. The vibrational amplitudes of the listed bond distances were refined as a group for each model; the values are 0.054(4) Å for Cb, 0.053(4) Å for Aa and Ab, 0.056(4) Å for Ca, 0.047(7) Å for Ba, and 0.045(10) Å for Da. Table 5 is the correlation matrix for some of the important parameters of the preferred model Cb. The Supporting Information includes a table with a complete list of distances and amplitudes for model Cb.

Discussion

Although model Cb is to be preferred based on the combined experimental electron-diffraction and theoretical data cited above, the structure itself raises important questions stemming from the length of the equatorial bond. At $r_a = 1.538$ ($2\sigma = 0.019$) Å this bond is about 0.06 Å longer than is predicted

theoretically and found experimentally in the solid state by neutron⁵ and X-ray diffraction.⁶ Table 6 affords a comparison of the bond lengths and ellipsoid dimensions from several of the experimental and theoretical studies. With the exception of the equatorial bond C₃₁–C₃₂ (and the bond C₉–C₃₁), all the bond distances from our work are 0.01–0.02 Å larger than the SCF values, in agreement with general experience in other cases. On the experimental side, again with the exception of C₃₁–C₃₂, our values are in excellent agreement with the results of both the neutron-diffraction and X-ray work. In view of the otherwise good agreement between our results and those from both theory and experiment, it is difficult to understand why the equatorial bonds are so much longer in the gas phase. Some degree of bond elongation is to be expected from the difference between the sample temperatures in ours and the other inves-

Table 6. Bond Lengths and Ellipsoid Dimensions from Various Studies of $C_{70}^{a,b}$

distance	experimental				theoretical	
	GED	SED ^c	ND ^d	X-ray ^e	SCF/	BP86/
					dzp	tzp
C ₁ –C ₂	1.461(8)	1.464(9)	1.460(4)	1.458(6)	1.451	1.454
C ₁ –C ₆	1.388(17)	1.37(1)	1.382(6)	1.380(4)	1.375	1.401
C ₆ –C ₇	1.453(11)	1.47(1)	1.449(5)	1.459(5)	1.446	1.450
C ₁₀ –C ₁₂	1.386(25)	1.37(1)	1.396(6)	1.370(4)	1.361	1.395
C ₇ –C ₈	1.468(11)	1.46(1)	1.464(7)	1.460(4)	1.457	1.449
C ₈ –C ₉	1.425(14)	1.47(+1,–3)	1.420(4)	1.430(4)	1.415	1.441
C ₉ –C ₃₁	1.405(13)	1.39(1)	1.415(5)	1.407(7)	1.407	1.424
C ₃₁ –C ₃₂	1.538(19)	1.41(+3,–1)	1.477(6)	1.476(5)	1.475	1.471
RR–EQ ^f	3.590(25)	3.47(3)	3.562(3)		3.542	3.571
Z ^g	3.953(32)	3.95(1)	3.984(2)		3.958	3.973
ref	this work	4	5	6	2	24

^a In angstroms. Values in parentheses are $2 \times$ esd for GED, unspecified for SED, and esd for ND and X-ray. ^b Distances from different methods should in principle differ slightly. ^c Solid-state electron diffraction. ^d Neutron diffraction at 300 K. ^e X-ray diffraction from $C_{70}S_{48}$. ^f Distance from the center of the molecule to an equatorial atom. ^g Distance from the center of the molecule to the center of a capping pentagon.

tigations, but the amount displayed by the equatorial bonds would be exceptional in all except floppy molecules subject to large-amplitude motion. However, there are large-amplitude vibrational motions, such as combinations of a boat-chair bends of the equatorial hexagons, which would mostly affect the lengths of the equatorial bonds. If the groups of 30 atoms above and below the equatorial belt were to have the dynamical stability of C_{60} of which they represent one-half, such motions might lead to substantial lengthening of the equatorial bonds without having much effect on the others.

There is, of course, the possibility that one of the other models is in fact nearer the truth than Cb. Models Aa, Ca, Ba, and Da all have short equatorial bonds (1.435(37), 1.423(39), 1.411(50), and 1.386(47) Å, respectively); however, they do not find the same support as Cb in terms of the agreement between the calculated and observed ^{13}C NMR shifts. Further, the equatorial distance in these models is even shorter than those measured in the solid and those calculated ab initio (Table 4). One aspect of the latter comparison is worth noting: taking into account the general experience that SCF distances at this level of ab initio theory are generally 0.01–0.02 Å shorter than experimental ones, model Cb provides a better match to the theoretical equatorial bond distance than do any of the others. A last point, seen in Table 5, is that the equatorial bond distance is only weakly correlated with the other parameters. Thus, small errors in these parameter values will have but little effect on the value of this distance.

Although there may be some uncertainty about the equatorial bond distance itself, the *average* length of the eight different bonds, $\langle C-C \rangle$, is well determined by our study. This quantity

evaluated over all six refined models is equal to 1.433₅ Å with an average deviation of 0.006₀ Å, a result that indicates $\langle C-C \rangle$ is almost completely independent of the refinement conditions. The average bond distances found in the solid state and calculated ab initio are expected to be slightly different from ours, first because the quantities being measured are not exactly the same and second because different thermal effects apply. From the data of Table 6 the ab initio values of $\langle C-C \rangle$ are found to be 1.423₄ (SCF/DZP) and 1.435₆ Å (BP86/TZP), and the experimental solid-state values are 1.42₅ (SED), 1.432₉ (ND), and 1.430₀ Å (X-ray). Both theoretical values—SCF with the customary offset (increase) of 0.01–0.02 Å and BP86 where a possible offset is unknown but surely smaller—are in excellent agreement with our GED values. Of the experimental values the one from neutron diffraction should lie closest to ours since the scattering in both cases is largely from the atomic nuclei. X-ray distances, which reflect the centers of average planetary electron density, are often smaller than GED values due to the anisotropic thermal motion of the nuclei. Expectation based on these ideas about the relative magnitudes of our $\langle C-C \rangle$ and the other experimental values is borne out.

Our structure, like the one from neutron diffraction,⁵ does not support the notion of a slight “pinching in” of the molecule at its equator as was suggested by the condensed-phase electron-diffraction work.⁴ In our structure the circle passing through the equatorial (e-type) atoms has a diameter of 7.180 Å, whereas the diameter of the adjacent circle of d-type atoms is 6.943 Å. (Other atom-circle diameters are 6.062, 4.853, and 2.486 Å for c-, b-, and a-type atoms.) It is noteworthy, however, that despite the larger equatorial diameter, each of the equatorial hexagons is concave outward in the sense of being bent about 10° around the equatorial line joining atoms across the hexagon.

Acknowledgment. This work was supported by the National Science Foundation under grants CHE88-10070 and CHE95-23581. We are indebted to Prof. Harry C. Dorn and Ms. Ofelia Chapa-Perez for assistance with the purification of the first C_{70} sample. M.B. thanks Prof. W. Thiel and the Fonds der Chemischen Industrie for support, Ms. K. Eichkorn for assistance with TURBOMOLE, and Dr. P. T. Brain for bringing the experimental problem to his attention. The theoretical calculations were carried out on IBM RS6000 workstations at the University and at the ETH, Zürich (C4 cluster).

Supporting Information Available: Tables of the averaged intensity data, all distances and vibrational amplitudes for model Cb, and the principal distances and bond, out-of-plane, and flap angles for each of the six converged models (5 pages). See any current masthead page for ordering and Internet access instructions.

JA970110E